

**Claudin-1 has tumor suppressive activity and is a direct target of RUNX3 in gastric epithelial cells**

Ti Ling Chang<sup>1</sup>, Kosei Ito<sup>2</sup>, Tun Kiat Ko<sup>1</sup>, Qiang Liu<sup>1</sup>, Manuel Salto-Tellez<sup>1</sup>, Khay Guan Yeoh<sup>3</sup>, Hiroshi Fukamachi<sup>4</sup>, and Yoshiaki Ito<sup>1,5</sup>

<sup>1</sup>Cancer Science Institute of Singapore, National University of Singapore, Singapore;

<sup>2</sup>Graduate School of Biomedical Sciences, Nagasaki University, Nagasaki, Japan;

<sup>3</sup>Department of Medicine, Faculty of Medicine, National University of Singapore, Singapore; <sup>4</sup>Department of Molecular Oncology, Tokyo Medical and Dental University,

Tokyo, Japan; <sup>5</sup>Institute of Molecular and Cell Biology, Proteos, Singapore.

K.I. initiated the study, and T.L.C. and K.I. conducted the *in vivo* and *in vitro* analyses. T.K.K. conducted the *in vitro* analyses. Q.L., M.S.-T., and K.G.Y. provided the human clinical materials. H.F. provided mouse tissues and GIF cells. K.I. and T.L.C. wrote the manuscript. K.I. and Y.I. supervised the project.

Corresponding authors:

Kosei Ito, PhD

Tel: +81-95-819-7754, Fax: +81095-819-7633, Email: itok@nagasaki-u.ac.jp

Yoshiaki Ito, MD, PhD

Tel: +65-6586-9646, Fax: +65-6779-1117, Email: itoy@imcb.a-star.edu.sg

Abbreviations used in this paper: EMT, epithelial-mesenchymal transition; ZO, zonula-occluden.

## Abstract

**Background & Aims:** The transcription factor RUNX3 is a gastric tumor suppressor. Tumorigenic *Runx3*<sup>-/-</sup> gastric epithelial cells attach weakly to each other, compared with non-tumorigenic, *Runx3*<sup>+/+</sup> cells. We aimed to identify RUNX3 target genes that promote cell–cell contact to improve our understanding of RUNX3’s role in suppressing gastric carcinogenesis.

**Methods:** We compared gene expression profiles of *Runx3*<sup>+/+</sup> and *Runx3*<sup>-/-</sup> cells and observed down-regulation of genes associated with cell–cell adhesion in *Runx3*<sup>-/-</sup> cells. Reporter, mobility shift, and chromatin immunoprecipitation assays were used to examine the regulation of these genes by RUNX3. Tumorigenesis assays and immunohistological analyses of human gastric tumors were performed to confirm the role of the candidate genes in gastric tumor development.

**Results:** Mobility shift and ChIP assays revealed that the promoter activity of the gene that encodes the tight junction protein claudin-1 was up-regulated via the binding of RUNX3 to the RUNX consensus sites. The tumorigenicity of gastric epithelial cells from *Runx3*<sup>-/-</sup> mice was significantly reduced by restoration of claudin-1 expression, whereas knockdown of claudin-1 increased the tumorigenicity of human gastric cancer cells. Concomitant expression of RUNX3 and claudin-1 was observed in human normal gastric epithelium and cancers.

**Conclusions:** The tight junction protein claudin-1 has gastric tumor suppressive activity and is a direct transcriptional target of RUNX3. Claudin-1 is downregulated during the epithelial–mesenchymal transition (EMT); RUNX3 might therefore act as a tumor suppressor to antagonize the EMT.

## Introduction

Gastric cancer remains a major public health problem worldwide. It is the most common epithelial malignancy and is the leading cause of cancer-related death in Asia and in parts of South America. It remains the second most frequently diagnosed malignancy worldwide and is a cause of 12% of all cancer-related deaths each year<sup>1, 2</sup>.

Various genetic and epigenetic alterations of tumor suppressor and tumor-related genes have been associated with the development and progression of gastric cancer. Mutations in *p53*<sup>3, 4</sup>, *E-cadherin*<sup>5</sup>, and in the transforming growth factor beta (TGF- $\beta$ ) receptor<sup>6</sup> are involved in gastric carcinogenesis. Oncogenic activation of  *$\beta$ -catenin* and *K-ras* and amplification of *c-erbB2* and *c-met* have also been reported to be involved in the process<sup>7</sup>. Microsatellite instability (MSI) was observed in 5–10% of diffuse and 15–40% of intestinal-type gastric cancer, which is mainly caused by the inactivation of *hMLH1*, via promoter hypermethylation<sup>8</sup>. Although many genes have been analyzed in attempts to understand the molecular bases of human gastric carcinogenesis, a restricted number of genes that carry frequent alterations have been identified to date.

The *Runt-related* (*RUNX*) gene has been documented to play a role in gastrointestinal carcinogenesis. *RUNX3* is 1 of the 3 Runt-domain transcription factors that function in the TGF- $\beta$ /SMAD signaling pathway, which is essential for developmental and physiological processes<sup>9, 10</sup>. We have shown that loss of *RUNX3* abrogates TGF- $\beta$  signaling and that *RUNX3* is inactivated in more than 80% of gastric cancers, not only by gene silencing but also by protein mislocalization<sup>11, 12</sup>. *RUNX3* directly up-regulates the cyclin-dependent kinase inhibitor, *p21*<sup>WAF1/Cip1</sup><sup>13</sup> and the

proapoptotic gene, *Bim*,<sup>14, 15</sup> in response to TGF- $\beta$  signaling and down-regulates *VEGF*<sup>16</sup>. We thus concluded that *RUNX3* is a gastric tumor suppressor gene that controls the growth, apoptosis, and differentiation of gastric epithelial cells<sup>17-20</sup>. Recently, *RUNX3* was found to form a ternary complex with  $\beta$ -catenin/TCF4 and to attenuate the oncogenic Wnt signaling activity in human and mouse intestinal tumors<sup>21</sup>. These results support the contention that *RUNX3* functions as a tumor suppressor in gastrointestinal tract carcinogenesis.

In a previous study, we found that mouse embryonic gastric epithelial cells (GIF cells) isolated from E16.5 *Runx3*<sup>-/-</sup>*p53*<sup>-/-</sup> mice are tumorigenic in nude mice, whereas GIF cells from *Runx3*<sup>+/+</sup>*p53*<sup>-/-</sup> mice are not<sup>11</sup>. Furthermore, *Runx3*<sup>-/-</sup> GIF cells attach weakly to each other and do not form any glandular structures when cultured on collagen gel, while *Runx3*<sup>+/+</sup> GIF cells formed simple columnar epithelia with occasional glandular structures<sup>19</sup>, which suggests that cell polarity and epithelial sheet formation could not be established in *Runx3*<sup>-/-</sup> gastric epithelial cells.

One of the structures involved in cell–cell adhesion is the tight junction. The proteins that participate in the formation of tight junctions include claudins, occludins, junctional adhesion molecules (JAM), zona occludens (ZO), AF-6 (afadin), and cingulin. Claudins interact directly with occludin, ZO-1, ZO-2, and ZO-3 and indirectly with AF-6 and the myosin-binding molecule cingulin. These protein–protein interactions promote the scaffolding of the tight junction transmembrane proteins, thus providing a link to the actin cytoskeleton for the transduction of regulatory signals to and from tight junctions<sup>22, 23</sup>. Because of this ability, tight junction proteins are believed to be involved in the regulation of proliferation, differentiation, and other cellular functions. Claudin-1 is the

main component of the tight junction family of proteins and its expression is often cell-type- and tissue-dependent<sup>24, 25</sup>. Expression of claudin-1 is negatively regulated by 2 related transcription factors, Snail and Slug, which are involved in the induction of epithelial-mesenchymal transition (EMT), which is a normal developmental process characterized by loss of cell adhesion and increased mobility; EMT is now considered to contribute to invasive and metastatic tumor growth<sup>26</sup>.

In this study, we examined the expression of a group of genes related to cell–cell adhesion, to identify RUNX3 target genes that function in cell adhesion and to understand their role in gastric carcinogenesis. We identified *claudin-1* as a novel downstream target of RUNX3. The identification of this target gene will contribute to the improvement of our understanding of the mechanism underlying *RUNX3*-mediated suppression of gastric carcinogenesis.

## Materials and Methods

### Cell lines and cell culture

The GIF cell lines were isolated from gastric epithelial tissues of 16.5 dpc. *Runx3*<sup>-/-</sup>*p53*<sup>-/-</sup> (GIF-5 and -14) and *Runx3*<sup>+/+</sup>*p53*<sup>-/-</sup> (GIF-9 and -13) mouse fetuses, as described previously<sup>11, 19</sup>. GIF cells were maintained in DMEM supplemented with 10% fetal bovine serum (FBS).

The SNU16 and SNU719 gastric cancer cell lines were maintained in RPMI-1640 medium supplemented with 10% FBS. AGS, MKN74, and 293T cells were cultured in DMEM supplemented with 10% FBS. SNU16 and SNU719 cells were treated with 3 ng/ml of TGF- $\beta$  and 1  $\mu$ g/ml of TGF- $\beta$  inhibitor (SB431542; GlaxoSmithKline Pharmaceuticals, Brentford Middlesex, United Kingdom) was used for SNU16.

SNU16 cells that expressed antisense DNA against human *RUNX3* or Flag-*RUNX3* stably were generated as described previously<sup>12, 15</sup>. SNU719 and MKN74 cells that expressed Flag-tagged human *RUNX3* stably were generated via transfection using Lipofectamine 2000 (Invitrogen, Carlsbad, CA) as reported previously<sup>15, 27</sup>, followed by selection using 1 mg/ml G-418 (Roche Diagnostics, Indianapolis, IN). SNU16 cells that expressed antisense DNA against human *claudin-1* stably were generated via transfection with the pcDNA3.1 vector (Invitrogen) containing the entire inverted open reading frame (ORF) of the human *claudin-1* gene (636 bp), followed by selection using 0.125 mg/ml Hygromycin (Invitrogen). The endogenous *RUNX3* in SNU719 cells was knocked down using shRNA targeting *RUNX3* (5'-tcagtagtgggtaccaatctt-3')<sup>21</sup> and control shRNA targeting *GFP* (5'-ggctacgtccaggagcgca-3'). GeneClip U1 Hairpin Cloning Systems

(Promega, Madison, WI) was used as the vector for transfection, and transfectants were selected using 1 mg/ml G-418. GIF-5 and GIF-14 cells that expressed claudin-1 stably were generated via transfection with the pcDNA3.1 vector containing the entire murine *claudin-1* ORF (636 bp)<sup>28</sup> using Fugene 6 (Roche Diagnostics), followed by selection using 0.125 mg/ml Hygromycin.

### **Reverse-transcription polymerase chain reaction and Western blotting**

Total RNA and complementary DNA (cDNA) were obtained using the RNeasy mini kit (QIAGEN, Hilde, Germany) and the Omniscript reverse transcription kit (QIAGEN), respectively. Semiquantitative reverse-transcription polymerase chain reaction (RT-PCR) for the detection of *claudin-1* and *GAPDH* was then carried out using the following PCR primers: 5'-CCAACGCGGGGCTGCAGCT-3' and 5'-TTGTTTTTCGGGGACAGGA-3' for *claudin-1*, and 5'-GGTCGGAGTCAACGGATTTGGTCG-3' and 5'-CCTCCGACGCCTGCTTCACCAC-3' for *GAPDH*. Quantitative RT-PCR was performed using the real-time TaqMan Fast Universal PCR Master Mix system on an ABI PRISM 7900HT instrument (Applied Biosystems, Foster City, CA) for the detection of *RUNX3* (Hs00231709\_m1; Applied Biosystems) and human *claudin-1* (Hs00221623\_m1; Applied Biosystems).

Western blotting was performed using anti-RUNX3 (R3-5G4<sup>12</sup>; Medical & Biological Laboratories [MBL], Nagoya, Japan), anti-claudin-1 (18-7362; Zymed, South San Francisco, CA), anti-claudin-2 (51-6100; Zymed), anti-claudin-3 (34-1700; Zymed), anti-claudin-4 (36-4800; Zymed), anti-claudin-7 (34-9100; Zymed), anti-claudin-11 (36-

4500; Zymed), anti-claudin-16 (34-5400; Zymed), anti-ZO-1 (61-7300; Zymed), anti-ZO-2 (71-1400; Zymed), anti-ZO-3 (36-4100; Zymed), anti-occludin (71-1500; Zymed), anti-E-cadherin (610181; BD Pharmingen, San Jose, CA), and anti- $\beta$ -actin (AC-15; Sigma, St Louis, MO) antibodies.

### **Reporter assay**

The promoter region of human *claudin-1*, 1.5kb upstream from the *claudin-1* transcription start site, was PCR-amplified from SNU16 genomic DNA using the primers 5'-CGGGGTACCCCTGGGATACAACACG-3' and 5'-CGAGCTCCCCAGGCTCGGGAAGTCTGAG-3'. The amplified DNA segment was cloned into the pGL3-Basic vector (E1751; Promega) between the KpnI and SacI restriction sites. Three RUNX binding sites were mutated using the QuickChange XL site-directed mutagenesis kit (Stratagene, La Jolla, CA). AGS cells were transfected with the reporter plasmids and a promoterless pRL-SV40 vector (Promega), in which the SV40 promoter was deleted. The Dual-Luciferase Reporter Assay System (Promega) was used to measure the luciferase activity of the reporter plasmids, which was normalized to the activity of the promoterless pRL-SV40 vector.

### **Xenografts using nude mice**

GIF-5, GIF-14, and SNU16 cells ( $5 \times 10^6$  cells each) were injected subcutaneously into the flanks and backs of nude mice. Sixty days after injection, tumors were dissected and weighed.

### **Immunohistochemistry and immunocytochemistry**

Mouse tissues were fixed with 4% paraformaldehyde, embedded in paraffin, and sectioned at 5  $\mu\text{m}$ . Human tissues were fixed with 10% neutral-buffered formalin, embedded in paraffin, and serially sectioned at 4  $\mu\text{m}$ . Rehydrated specimens were treated for 40 min at 96°C with an antigen retrieval solution (S1700; DAKO, Glostrup, Denmark). The specimens were incubated with anti-claudin-1 (18-7362; Zymed) or anti-RUNX3 (R3-6E9<sup>12</sup>; MBL) antibodies. The EnVision+ system (K4010; DAKO) was used for visualization of signals.

Cells cultured on glass slides were incubated with rabbit anti-claudin-1 (18-7362; Zymed) antibody. Biotinylated anti-rabbit immunoglobulin G (IgG) (BA-1000; VECTOR Laboratories, Burlingame, CA) and fluorescein-conjugated avidin D (A-2001; VECTOR Laboratories) were subsequently used for immunofluorescence imaging.

### **Gastric cancer specimens**

Fifty-two gastric adenocarcinoma samples and corresponding non-cancerous tissues were obtained from the Department of Pathology and Surgery of the National University of Singapore, under a protocol approved by the Institutional Review Board.

### **Electrophoresis mobility shift assay**

Electrophoresis mobility shift assay (EMSA) was performed using the LightShift Chemiluminescent EMSA kit and a Chemiluminescent Nucleic Acid Detection Module (Pierce Biotechnology, Rockford, IL). Nuclear extracts from 293T cells expressing Flag-tagged RUNX3 were prepared using NE-PER Nuclear and Cytoplasmic Extraction

Reagents (Pierce Biotechnology). For supershift of bands, anti-RUNX3 (R3-5G4; MBL) antibody or mouse normal IgG were added after the binding reaction. The following oligonucleotides were used as labeled or unlabeled probes; 5'-CTTCCCCTCCCACCACACTCGCACC-3' (wild-type RUNX site [W]) and 5'-CTTCCCCTCCCATTACACTCGCACC-3' (mutated RUNX site [M]) for site 1, 5'-ACACTCGCACCACACACAAAAAGCA-3' (W) and 5'-ACACTCGCATTACACACAAAAAGCA-3' (M) for site 2, and 5'-TTCAATGATTCTTAACCACAACAGCACTTCTGACT-3' (W) and 5'-TTCAATGATTCTTAATTACAACAGCACTTCTGACT-3' (M) for site 3. The 5' end of the site 1 and 3 probes and the 3' end of the site 2 probe were biotinylated.

### **Chromatin immunoprecipitation assay**

Chromatin immunoprecipitation (ChIP) was performed using the chromatin immunoprecipitation assay kit (Upstate) with the anti-RUNX3 antibody (R3-6E9; MBL) or mouse normal IgG (sc-2025; Sigma). The primers used to amplify the DNA fragment were designed to comprise all three RUNX binding sites (sites 1-3): 5'-AAAACCATAGAAGCTTCCCCTCCC-3' and 5'-CCTCTATGTTTCTCAAAGCTTCC-3'.

## Results

### **RUNX3 mediates claudin-1 expression**

*Runx3*<sup>-/-</sup> gastric epithelial cells attached weakly to each other in collagen gel culture *in vitro*, which suggests the RUNX3 mediates expression of genes responsible for cell–cell contact and for formation of epithelial cell sheets<sup>19</sup>. To identify RUNX3 target genes involved in cell–cell contact, first we compared the gene expression profile of *Runx3*<sup>+/+</sup> (GIF-9) and *Runx3*<sup>-/-</sup> (GIF-5) cells. As shown in S.Table 1, we found that the expression of tight junction genes was generally reduced in *Runx3*<sup>-/-</sup> cells. As revealed by Western blot analysis, claudin-1, claudin-3, ZO-3, and occludin were highly expressed in the *Runx3*<sup>+/+</sup> GIF-9 and -13 cells, whereas no expression or very low levels of these proteins were detected in the *Runx3*<sup>-/-</sup> GIF-5 and -14 cells (Fig. 1A). Claudin-2, -4, -7, -11, and -16 were not detected in any of the GIF cell lines, as assessed by Western blotting (data not shown). Inactivation of E-cadherin has been reported in diffuse type gastric cancer<sup>5</sup>; however, its level of expression was similar in all GIF cells, regardless of *Runx3* state.

To identify genuine direct targets of RUNX3 among the genes encoding tight junction proteins, we used the human gastric cancer-derived SNU16 cell line, in which we can conditionally activate RUNX3 function. RUNX3 is inactive in the cytoplasm of SNU16 cells; however, it becomes functional when translocated into the nucleus via TGF- $\beta$  treatment<sup>12, 15</sup>. Among the tight junction proteins tested, only claudin-1 was up-regulated in a time-dependent manner after addition of TGF- $\beta$  to SNU16 cells (Fig. 1B). This up-regulation was abrogated in the presence of the TGF- $\beta$  inhibitor (Fig. 1C). The

knockdown of RUNX3 abolished this TGF- $\beta$ -mediated up-regulation of claudin-1, at both the protein and the mRNA levels (Fig. 1D). Furthermore, the knockdown of RUNX3 in SNU719 cells which express endogenous RUNX3 at a low level inhibited the TGF- $\beta$ -induced claudin-1 expression as well (Fig. 1E). The results show TGF- $\beta$ -dependent and RUNX3-mediated induction of claudin-1 in SNU16 and SNU719 cells. On the other hand, overexpression of exogenous RUNX3 up-regulated claudin-1 in SNU719 and a *RUNX3*-negative cell line, MKN74<sup>12, 27</sup> (Fig. 1F). These results suggest that *claudin-1* is a strong RUNX3 target gene candidate and that its expression is positively regulated by RUNX3 in gastric epithelial cells.

Consistent with these results, claudin-1 was clearly immunodetected at the cellular membrane in *Runx3*<sup>+/+</sup> cells (e.g., GIF-9, -13, and wild-type mouse gastric epithelial cells), but not in *Runx3*<sup>-/-</sup> cells (e.g., GIF-5, -14, and *Runx3*<sup>-/-</sup> mouse cells) (Fig. 2A, B). Thus, for all follow-up experiments, we focused on the elucidation of the mechanism underlying the RUNX3-mediated regulation of *claudin-1* expression.

### ***Claudin-1* is a direct target of RUNX3**

We found that the human *claudin-1* promoter region between nucleotides -1176 and -1080 is highly homologous (81%) to that of the mouse *claudin-1* promoter and that it contains three RUNX consensus binding sites (sites 1-3; Fig. 3A). To examine the regulation of human *claudin-1* expression by RUNX3 through consensus binding sites, we generated a luciferase reporter construct encompassing 1.5 kb of sequence upstream from the human *claudin-1* transcription start site (Fig. 3B). The three RUNX consensus sites were mutated in turn, as shown in Fig. 3B, and seven types of reporter plasmids,

termed M1, M2, M3, M1+2, M1+3, M2+3, and M1+2+3, as well as the wild-type (WT) promoter construct, were subjected to reporter assays using the *RUNX3*-negative cell line AGS. RUNX3 forms complexes with Smads to stimulate transcription of target genes in a cooperative manner after stimulation by TGF- $\beta$ <sup>9, 13, 29</sup>. We found that the 1.5 kb human *claudin-1* WT promoter was activated by exogenous RUNX3 and was enhanced by coexpression of RUNX3 with Smad3 and Smad4 (Fig. 3C). The activation of the 1.5 kb human *claudin-1* promoter depended on the three RUNX consensus sites, as shown in Fig. 3D.

The direct binding of RUNX3 to the consensus sites in the *claudin-1* promoter was confirmed using the EMSA and ChIP assays. As shown in Fig. 3E, RUNX3 specifically bound to the three RUNX consensus sites, as shown by EMSA, and its binding was significantly enhanced by TGF- $\beta$  treatment, as revealed by ChIP assay (Fig. 3F). These results suggest that *claudin-1* expression is directly regulated by RUNX3 in gastric epithelial cells.

### **Restoration of claudin-1 expression suppresses *Runx3*<sup>-/-</sup> tumorigenicity in nude mice**

In a previous study, we showed that GIF cells from *Runx3*<sup>-/-</sup>*p53*<sup>-/-</sup> mouse gastric epithelium are tumorigenic in nude mice, whereas those of *Runx3*<sup>+/+</sup>*p53*<sup>-/-</sup> mice are not<sup>11</sup>. As shown in Figs 1A and 2A, the *Runx3*<sup>-/-</sup> GIF-5 and -14 cells expressed claudin-1 at very low or negligible levels. To assess whether claudin-1 acts as a tumor suppressor in gastric epithelial cells, we generated GIF-5 and -14 cells stably expressing exogenous claudin-1 (Fig. 4D) and examined their tumorigenicity by inoculating them into nude mice. The restoration of exogenous claudin-1 expression greatly suppressed the

tumorigenicity of *Runx3*<sup>-/-</sup> cells and this tumor suppressive effect was correlated with the level of expression of claudin-1 in these cell lines (Fig. 4A, B, D).

Conversely, we examined the effect of claudin-1 knockdown on the tumorigenesis of human gastric epithelial cells. We transfected SNU16 cells with antisense DNA against human *claudin-1* and obtained stable cell lines in which the level of *claudin-1* was significantly reduced. The tumorigenicity of these SNU16 cells was inversely correlated with the level of expression of claudin-1 (Fig. 4D). These observations collectively show that claudin-1 has tumor suppressive activity in gastric epithelial cells.

#### **The expression of claudin-1 and RUNX3 is highly correlated in normal human gastric epithelia and human gastric cancers**

The expression patterns of RUNX3 and claudin-1 in normal gastric epithelium were immunohistochemically examined. Claudin-1 was strongly expressed in surface epithelial cells and chief cells, but was weakly expressed in parietal cells (Fig. 5). RUNX3 was immunodetected in the nucleus of surface epithelial cells and in the nucleus and cytoplasm of chief cells, as reported previously<sup>12</sup>. These results demonstrate that the expression of claudin-1 and RUNX3 is highly correlated in normal human gastric mucosa.

We also examined the expression of these proteins in human gastric cancers. Among the 52 gastric cancer samples tested here, 29 (56%) were intestinal and 23 (44%) were diffuse types. Thirty-seven samples (71%) exhibited RUNX3 inactivation (Table 1). Nucleus RUNX3 expression was scored as positive, whereas no or cytoplasmic RUNX3 expression were scored as negative. Fifteen samples were both RUNX3- and claudin-1-positive (29%; Figure 6A and Table 1), 17 cases were negative for both (33%; Figure 6B

and Table 1), and 20 cases were RUNX3-negative but claudin-1-positive (38%; Table 1). However, no RUNX3-positive and claudin-1-negative cases were found (Table 1). This observation suggests that claudin-1 is a positive target of RUNX3 and that factors other than RUNX3 are also likely to participate in stimulating its expression. SNU16 and SNU719 cells in the absence of TGF- $\beta$  (Fig. 1B-E) and *RUNX3*-negative MKN74 cells (Fig. 1F) showed the basal level of claudin-1 expression. The mechanism of regulation of claudin-1 expression by the factors other than RUNX3 remains to be studied. Interestingly, however, in the absence of RUNX3 expression, claudin-1 expression appeared less intense when compared with RUNX3-positive cases in all 3 types of gastric cancers analyzed (Fig. 6C).

Taken together, these observations show that claudin-1 is a positive target of RUNX3 in gastric epithelial cells.

## Discussion

In the present study, we examined the possible mechanism via which RUNX3, a transcription factor and a potent gastric cancer tumor suppressor, regulates cell–cell adhesion. We found that a major tight junction protein, claudin-1, is transcriptionally regulated by RUNX3. Furthermore, exogenous expression of claudin-1 suppressed tumor growth and knockdown of claudin-1 expression enhanced tumor growth. Thus, we concluded that claudin-1 has tumor suppressive activity and is a direct target of RUNX3.

Approximately 75% of our Runx3 knockout mice died during the first day after birth because of starvation, and none of the mice with the C57BL/6 genetic background survived beyond 10 days<sup>11</sup>. We also observed a characteristic wrinkled skin appearance in our Runx3 knockout mice, similar to that observed in the *claudin-1* knockout mice (data not shown). The wrinkled skin appearance, which is a result of the loss of epidermal barrier function, leads to death of the *claudin-1* knockout mice within 1 day after birth<sup>30</sup>. Therefore, it is possible that *Runx3*<sup>-/-</sup> mice also die from the loss of epidermal barrier function in the skin.

RUNX3 has been shown to contribute to tumor suppressor activity as a component of the TGF- $\beta$  tumor suppressor pathway<sup>9</sup> through the attenuation of cell growth with a CDK inhibitor<sup>13</sup>, induction of apoptosis<sup>15</sup>, and inhibition of angiogenesis<sup>16</sup> and metastasis<sup>31</sup> in gastric cancers. Here, we showed that RUNX3 also exerts its tumor suppressor activity by regulating tight junction function in gastric cancer. Thus, RUNX3 may play a central role in the suppression of tumorigenesis, not only by coordinating

various signaling pathways but also by controlling cell morphology and tissue structures via the regulation of tight junction protein expression.

One of the most exciting developments in the field of cancer research in recent years is the concept of cancer stem cells and their relationship to EMT. The cell–cell contact is usually loosened in cancer cells and epithelial cells acquire mesenchymal cell properties. Snail and Slug are activated by oncogenic stimuli, which in turn repress E-cadherin expression to induce EMT<sup>32, 33</sup>. Recently, claudin-1 was also shown to be negatively and positively regulated by Snail/Slug<sup>34</sup> and p63, respectively, which function primarily in epithelial–mesenchymal development during embryogenesis<sup>35</sup>. This suggests that reduction of claudin-1 expression is a part of the EMT process. As we found that claudin-1 is positively regulated by RUNX3, the tumor suppressor function of RUNX3 may be, at least in part, to inhibit induction of EMT and, perhaps, cancer stem cells.

RUNX3 was found to positively regulate the expression of claudin-1. However, RUNX3 did not alter the expression of E-cadherin. The von Hippel-Lindau (*VHL*) tumor suppressor gene was shown recently to regulate claudin-1 and occludin, without involving E-cadherin<sup>36</sup>. The similarity between the *VHL* and *RUNX3* tumor suppressor genes in this respect suggests that tight junction proteins are important tumor suppressor targets and loss of tumor suppressors with concomitant loss of tight junction proteins suggests the importance of tight junction proteins and perhaps EMT in carcinogenic processes.

In many types of cancers, TGF- $\beta$  plays a complex dual role. At early stages of epithelial neoplasia the TGF- $\beta$  pathway functions as a tumor suppressor, inhibiting primary tumor growth and inducing apoptosis. At later stages of carcinogenesis, however,

tumor cells that have developed the ability to bypass these tumor suppressor functions may use TGF- $\beta$  for tumor progression and invasion, promoting EMT<sup>37</sup>. RUNX3 functions as a tumor suppressor under the TGF- $\beta$ -signalling pathway<sup>9</sup>. In this study, we used SNU16 and SNU719 cell lines sensitive to cell growth-inhibitory and apoptosis-inducing action of TGF- $\beta$ <sup>13, 15</sup>. Using the system for examining the tumor suppressive TGF- $\beta$  function in early stages of epithelial neoplasia, we successfully demonstrated the up-regulation of claudin-1.

Expression of claudin family in gastric and other cancers has been studied by many laboratories but the results are conflicting. Although some investigators observed that claudin-1,-3,-4,-5 and -7 are reduced in diffuse type gastric cancer<sup>38-40</sup>, up-regulation of claudin-7 in intestinal type has also been reported<sup>39, 40</sup>. Reports on the expression of claudin family in other types of cancer are also controversial. In breast cancer, decreased expression of claudin-1 and -7 was reported<sup>41</sup>, but increased claudin-1 and -4 expression in the basal-like subtype<sup>42</sup> and increased claudin-4 expression in poor prognosis and high tumor grade<sup>43</sup> were also published. In colon cancer, while decreased expression of claudin-1 was reported to be associated with higher tumor grade<sup>44</sup>, an opposite conclusion has also been reported<sup>45</sup>. A possible cause of this controversy may be a reflection of the complexity of cancer cells. For example, claudin-7 is shown to be associated with EpCAM<sup>46</sup>. Association of cellular proteins to claudins in some cases, but not in other cases, might change the antigenicity of claudins. Some investigators reported the expression by semi-quantitative manner, whereas others described simply in a positive or negative fashion. To avoid conflicting results, precise mechanisms of

regulation of each claudin expression and their subcellular localization would have to be studied.

In the present study, we found that claudin-1 is a direct target of RUNX3. The latter is deeply involved in the TGF- $\beta$ -signaling pathway, which is well related to gastric carcinogenesis. The stage of carcinogenesis at which the expression of claudin-1 is down-regulated and how this correlates with other signaling cascades (e.g., oncogenic Wnt signaling) remain to be determined.

## **Acknowledgments**

We thank Dr Eveline Schneeberger for providing the murine *claudin-1* cDNA and Tomoko Ito and Kotaro Tada for technical assistance.

## **Conflicts of interest**

The authors disclose no conflicts.

## **Funding**

Supported by the Agency for Science, Technology, and Research, Singapore, by the Singapore Millenium Foundation scholarship (to T.L.C.), and by the Special Coordination Funds for Promoting Science and Technology of the Ministry of Education, Culture, Sports, Science, and Technology, Japan (to K.I.).

## References

1. Parkin DM, Pisani P, Ferlay J. Global cancer statistics. *CA Cancer J Clin* 1999;49:33-64, 1.
2. Zheng L, Wang L, Ajani J, Xie K. Molecular basis of gastric cancer development and progression. *Gastric Cancer* 2004;7:61-77.
3. Tamura G, Kihana T, Nomura K, Terada M, Sugimura T, Hirohashi S. Detection of frequent p53 gene mutations in primary gastric cancer by cell sorting and polymerase chain reaction single-strand conformation polymorphism analysis. *Cancer Res* 1991;51:3056-8.
4. Kim IJ, Kang HC, Shin Y, Park HW, Jang SG, Han SY, Lim SK, Lee MR, Chang HJ, Ku JL, Yang HK, Park JG. A TP53-truncating germline mutation (E287X) in a family with characteristics of both hereditary diffuse gastric cancer and Li-Fraumeni syndrome. *J Hum Genet* 2004;49:591-5.
5. Guilford P, Hopkins J, Harraway J, McLeod M, McLeod N, Harawira P, Taite H, Scoular R, Miller A, Reeve AE. E-cadherin germline mutations in familial gastric cancer. *Nature* 1998;392:402-5.
6. Park K, Kim SJ, Bang YJ, Park JG, Kim NK, Roberts AB, Sporn MB. Genetic changes in the transforming growth factor beta (TGF-beta) type II receptor gene in human gastric cancer cells: correlation with sensitivity to growth inhibition by TGF-beta. *Proc Natl Acad Sci U S A* 1994;91:8772-6.
7. Ushijima T, Sasako M. Focus on gastric cancer. *Cancer Cell* 2004;5:121-5.
8. Fang DC, Wang RQ, Yang SM, Yang JM, Liu HF, Peng GY, Xiao TL, Luo YH. Mutation and methylation of hMLH1 in gastric carcinomas with microsatellite instability. *World J Gastroenterol* 2003;9:655-9.
9. Ito Y, Miyazono K. RUNX transcription factors as key targets of TGF-beta superfamily signaling. *Curr Opin Genet Dev* 2003;13:43-7.
10. Ito Y. RUNX genes in development and cancer: regulation of viral gene expression and the discovery of RUNX family genes. *Adv Cancer Res* 2008;99:33-76.
11. Li QL, Ito K, Sakakura C, Fukamachi H, Inoue K, Chi XZ, Lee KY, Nomura S, Lee CW, Han SB, Kim HM, Kim WJ, Yamamoto H, Yamashita N, Yano T, Ikeda T, Itohara S, Inazawa J, Abe T, Hagiwara A, Yamagishi H, Ooe A, Kaneda A, Sugimura T, Ushijima T, Bae SC, Ito Y. Causal relationship between the loss of RUNX3 expression and gastric cancer. *Cell* 2002;109:113-24.
12. Ito K, Liu Q, Salto-Tellez M, Yano T, Tada K, Ida H, Huang C, Shah N, Inoue M, Rajnakova A, Hiong KC, Peh BK, Han HC, Ito T, Teh M, Yeoh KG, Ito Y. RUNX3, a novel tumor suppressor, is frequently inactivated in gastric cancer by protein mislocalization. *Cancer Res* 2005;65:7743-50.
13. Chi XZ, Yang JO, Lee KY, Ito K, Sakakura C, Li QL, Kim HR, Cha EJ, Lee YH, Kaneda A, Ushijima T, Kim WJ, Ito Y, Bae SC. RUNX3 suppresses gastric epithelial cell growth by inducing p21(WAF1/Cip1) expression in cooperation with transforming growth factor {beta}-activated SMAD. *Mol Cell Biol* 2005;25:8097-107.

14. Yamamura Y, Lee WL, Inoue K, Ida H, Ito Y. RUNX3 cooperates with FoxO3a to induce apoptosis in gastric cancer cells. *J Biol Chem* 2006;281:5267-76.
15. Yano T, Ito K, Fukamachi H, Chi XZ, Wee HJ, Inoue K, Ida H, Bouillet P, Strasser A, Bae SC, Ito Y. The RUNX3 tumor suppressor upregulates Bim in gastric epithelial cells undergoing transforming growth factor beta-induced apoptosis. *Mol Cell Biol* 2006;26:4474-88.
16. Peng Z, Wei D, Wang L, Tang H, Zhang J, Le X, Jia Z, Li Q, Xie K. RUNX3 inhibits the expression of vascular endothelial growth factor and reduces the angiogenesis, growth, and metastasis of human gastric cancer. *Clin Cancer Res* 2006;12:6386-94.
17. Fukamachi H. Runx3 controls growth and differentiation of gastric epithelial cells in mammals. *Dev Growth Differ* 2006;48:1-13.
18. Fukamachi H, Ito K. Growth regulation of gastric epithelial cells by Runx3. *Oncogene* 2004;23:4330-5.
19. Fukamachi H, Ito K, Ito Y. Runx3<sup>-/-</sup> gastric epithelial cells differentiate into intestinal type cells. *Biochem Biophys Res Commun* 2004;321:58-64.
20. Ito K, Inoue KI, Bae SC, Ito Y. Runx3 expression in gastrointestinal tract epithelium: resolving the controversy. *Oncogene* 2009;28:1379-84.
21. Ito K, Lim AC, Salto-Tellez M, Motoda L, Osato M, Chuang LS, Lee CW, Voon DC, Koo JK, Wang H, Fukamachi H, Ito Y. RUNX3 attenuates beta-catenin/T cell factors in intestinal tumorigenesis. *Cancer Cell* 2008;14:226-37.
22. Furuse M, Tsukita S. Claudins in occluding junctions of humans and flies. *Trends Cell Biol* 2006;16:181-8.
23. Cordenonsi M, D'Atri F, Hammar E, Parry DA, Kendrick-Jones J, Shore D, Citi S. Cingulin contains globular and coiled-coil domains and interacts with ZO-1, ZO-2, ZO-3, and myosin. *J Cell Biol* 1999;147:1569-82.
24. Tepass U. Claudin complexities at the apical junctional complex. *Nat Cell Biol* 2003;5:595-7.
25. Tsukita S, Yamazaki Y, Katsuno T, Tamura A. Tight junction-based epithelial microenvironment and cell proliferation. *Oncogene* 2008;27:6930-8.
26. Mani SA, Guo W, Liao MJ, Eaton EN, Ayyanan A, Zhou AY, Brooks M, Reinhard F, Zhang CC, Shipitsin M, Campbell LL, Polyak K, Brisken C, Yang J, Weinberg RA. The epithelial-mesenchymal transition generates cells with properties of stem cells. *Cell* 2008;133:704-15.
27. Guo WH, Weng LQ, Ito K, Chen LF, Nakanishi H, Tatematsu M, Ito Y. Inhibition of growth of mouse gastric cancer cells by Runx3, a novel tumor suppressor. *Oncogene* 2002;21:8351-5.
28. McCarthy KM, Francis SA, McCormack JM, Lai J, Rogers RA, Skare IB, Lynch RD, Schneeberger EE. Inducible expression of claudin-1-myc but not occludin-VSV-G results in aberrant tight junction strand formation in MDCK cells. *J Cell Sci* 2000;113 Pt 19:3387-98.
29. Hanai J, Chen LF, Kanno T, Ohtani-Fujita N, Kim WY, Guo WH, Imamura T, Ishidou Y, Fukuchi M, Shi MJ, Stavnezer J, Kawabata M, Miyazono K, Ito Y. Interaction and functional cooperation of PEBP2/CBF with Smads. Synergistic induction of the immunoglobulin germline Calpha promoter. *J Biol Chem* 1999;274:31577-82.

30. Furuse M, Hata M, Furuse K, Yoshida Y, Haratake A, Sugitani Y, Noda T, Kubo A, Tsukita S. Claudin-based tight junctions are crucial for the mammalian epidermal barrier: a lesson from claudin-1-deficient mice. *J Cell Biol* 2002;156:1099-111.
31. Sakakura C, Hasegawa K, Miyagawa K, Nakashima S, Yoshikawa T, Kin S, Nakase Y, Yazumi S, Yamagishi H, Okanoue T, Chiba T, Hagiwara A. Possible involvement of RUNX3 silencing in the peritoneal metastases of gastric cancers. *Clin Cancer Res* 2005;11:6479-88.
32. Battle E, Sancho E, Franci C, Dominguez D, Monfar M, Baulida J, Garcia De Herreros A. The transcription factor snail is a repressor of E-cadherin gene expression in epithelial tumour cells. *Nat Cell Biol* 2000;2:84-9.
33. Cano A, Perez-Moreno MA, Rodrigo I, Locascio A, Blanco MJ, del Barrio MG, Portillo F, Nieto MA. The transcription factor snail controls epithelial-mesenchymal transitions by repressing E-cadherin expression. *Nat Cell Biol* 2000;2:76-83.
34. Martinez-Estrada OM, Culleres A, Soriano FX, Peinado H, Bolos V, Martinez FO, Reina M, Cano A, Fabre M, Vilaro S. The transcription factors Slug and Snail act as repressors of Claudin-1 expression in epithelial cells. *Biochem J* 2006;394:449-57.
35. Lopardo T, Lo Iacono N, Marinari B, Giustizieri ML, Cyr DG, Merlo G, Crosti F, Costanzo A, Guerrini L. Claudin-1 is a p63 target gene with a crucial role in epithelial development. *PLoS ONE* 2008;3:e2715.
36. Harten SK, Shukla D, Barod R, Hergovich A, Balda MS, Matter K, Esteban MA, Maxwell PH. Regulation of renal epithelial tight junctions by the von Hippel-Lindau tumor suppressor gene involves occludin and claudin 1 and is independent of E-cadherin. *Mol Biol Cell* 2009;20:1089-101.
37. Massague J. TGFbeta in Cancer. *Cell* 2008;134:215-30.
38. Soini Y, Tommola S, Helin H, Martikainen P. Claudins 1, 3, 4 and 5 in gastric carcinoma, loss of claudin expression associates with the diffuse subtype. *Virchows Arch* 2006;448:52-8.
39. Johnson AH, Frierson HF, Zaika A, Powell SM, Roche J, Crowe S, Moskaluk CA, El-Rifai W. Expression of tight-junction protein claudin-7 is an early event in gastric tumorigenesis. *Am J Pathol* 2005;167:577-84.
40. Park JY, Park KH, Oh TY, Hong SP, Jeon TJ, Kim CH, Park SW, Chung JB, Song SY, Bang S. Up-regulated claudin 7 expression in intestinal-type gastric carcinoma. *Oncol Rep* 2007;18:377-82.
41. Hoevel T, Macek R, Swisshelm K, Kubbies M. Reexpression of the TJ protein CLDN1 induces apoptosis in breast tumor spheroids. *Int J Cancer* 2004;108:374-83.
42. Blanchard AA, Skliris GP, Watson PH, Murphy LC, Penner C, Tomes L, Young TL, Leygue E, Myal Y. Claudins 1, 3, and 4 protein expression in ER negative breast cancer correlates with markers of the basal phenotype. *Virchows Arch* 2009;454:647-56.
43. Lanigan F, McKiernan E, Brennan DJ, Hegarty S, Millikan RC, McBryan J, Jirstrom K, Landberg G, Martin F, Duffy MJ, Gallagher WM. Increased claudin-4

- expression is associated with poor prognosis and high tumour grade in breast cancer. *Int J Cancer* 2009;124:2088-97.
44. Resnick MB, Konkin T, Routhier J, Sabo E, Pricolo VE. Claudin-1 is a strong prognostic indicator in stage II colonic cancer: a tissue microarray study. *Mod Pathol* 2005;18:511-8.
  45. Dhawan P, Singh AB, Deane NG, No Y, Shiou SR, Schmidt C, Neff J, Washington MK, Beauchamp RD. Claudin-1 regulates cellular transformation and metastatic behavior in colon cancer. *J Clin Invest* 2005;115:1765-76.
  46. Nubel T, Preobraschenski J, Tuncay H, Weiss T, Kuhn S, Ladwein M, Langbein L, Zoller M. Claudin-7 regulates EpCAM-mediated functions in tumor progression. *Mol Cancer Res* 2009;7:285-99.

## Figure Legends

**Figure 1.** RUNX3 mediates the TGF- $\beta$ -induced expression of claudin-1.

(A) Expression of the indicated tight junction proteins and E-cadherin in the *Runx3*<sup>-/-</sup> GIF-5 and -14 cells and in the *Runx3*<sup>+/+</sup> GIF-9 and -13 cells, as revealed by Western blot analysis.

(B) Induction of the expression of the indicated tight junction proteins and E-cadherin by TGF- $\beta$  in SNU16 cells, as revealed by Western blot analysis.

(C) Abolishment of the TGF- $\beta$ -induced claudin-1 expression by the TGF- $\beta$  inhibitor in SNU16 cells, as revealed by Western blot analysis.

(D) The TGF- $\beta$ -induced claudin-1 expression was inhibited by RUNX3 knockdown in SNU16 cells, as revealed by RT-PCR and Western blot analyses. RUNX3 was knocked down using an antisense DNA against *RUNX3* (AS-SNU16).

(E) The TGF- $\beta$ -induced claudin-1 expression was inhibited by RUNX3 knockdown in SNU719 cells, as revealed by Western blot analyses. RUNX3 was knocked down using a shRNA targeting *RUNX3* (sh-RUNX3). A shRNA targeting *GFP* (sh-GFP) was used as a control.

(F) Up-regulation of claudin-1 by exogenous Flag-tagged RUNX3 (Flag-RUNX3) in SNU719 and MKN74 cells, as revealed by Western blot analyses. The exogenous Flag-RUNX3 (exo) and endogenous RUNX3 (endo) were detected using an anti-RUNX3 antibody (R3-5G4) in SNU719 cells. Cells were transfected with the pcDNA3 as a control (Vector).

**Figure 2.** Claudin-1 is expressed in *Runx3*<sup>+/+</sup> cells but not in *Runx3*<sup>-/-</sup> cells, both *in vivo* and *in vitro*.

(A) Expression of claudin-1 in *Runx3*<sup>+/+</sup> GIF-9 and -13 cells but not in *Runx3*<sup>-/-</sup> GIF-5 and -14 cells *in vitro*, as assessed by immunocytochemical analysis.

(B) Expression of claudin-1 in wild-type (WT) but not in *Runx3*<sup>-/-</sup> (-/-) samples from the stomach of neonatal mice *in vivo*, as revealed by immunocytochemical analysis. Specimens were counterstained with hematoxylin. Scale bars, 100  $\mu$ m.

**Figure 3.** RUNX3 regulates claudin-1 expression through the RUNX consensus sites present in its promoter.

(A) Three RUNX consensus sites (sites 1–3) are located in the highly conserved *claudin-1* promoter region. The figure shows nucleotides –1176 to –1080 of the human *claudin-1* promoter.

(B) Mutations (M1 to M3) were introduced in the RUNX consensus sites, upstream from the human *claudin-1* transcriptional start site.

(C) The *Claudin-1* promoter was activated by RUNX3 and was enhanced by coexpression of RUNX3 with Smad3 and Smad4 in AGS cells. The luciferase activity was normalized to the activity of the promoterless pRL-SV40 vector, which was used as an internal control.

(D) Activity of the WT and of the seven mutant reporter constructs (M1, M2, M3, M1+2, M1+3, M2+3, and M1+2+3) shown in panel B in AGS cells. AGS cells were cotransfected with the control vector or with expression vectors for RUNX3 and/or

Smad3 and Smad4. The luciferase activity was normalized to the activity of the promoterless pRL-SV40 vector, which was used as an internal control.

(E) Direct binding of RUNX3 to the three RUNX consensus sites (sites 1–3; see panel A) in the promoter, as revealed by EMSA. The nuclear extracts of 293T cells expressing exogenous RUNX3 (+) or the empty control vector (–) were incubated with the wild-type (W) and RUNX site-mutated (M) probes. To shift the RUNX3/probe complexes, an anti-RUNX3 antibody (R3-5G4;  $\alpha$ R3) and a normal mouse IgG (IgG) were added. The RUNX3/probe complexes (arrow), bands shifted by the anti-RUNX3 antibody (SS), and non-specific bands (asterisk) were detected.

(F) Direct binding of RUNX3 to the RUNX consensus sites in the promoter, as revealed by ChIP analysis. TGF- $\beta$ -treated SNU16 cells were subjected to ChIP analysis using an anti-RUNX3 antibody or a normal murine IgG. DNA precipitates were PCR-amplified (30, 32, or 35 cycles) using primers for the human *claudin-1* promoter region (which contains three RUNX consensus sites) or for *GAPDH*, which was used as an internal control.

**Figure 4.** Tumor suppressive effect of claudin-1 in gastric epithelial cells.

(A and B) Weight of tumors formed by *Runx3*<sup>-/-</sup> GIF-5 (A) and -14 (B) cells transfected with plasmids expressing mouse *claudin-1* (clones 1 and 2; Cl-1 and -2). GIF-5 and -14 cells expressing the empty vector (pcDNA3) were used as controls.

(C) Weight of tumors formed by SNU16 cells. SNU16 cells stably expressing an antisense DNA against human *claudin-1* (clones 1 and 2; AS-Cl-1 and -2) and control SNU16 cells expressing the empty vector (pcDNA3) were inoculated into nude mice.

(D) Expression of exogenous mouse claudin-1 in GIF-5 and -14 cells and of endogenous human claudin-1 in SNU16 cells, as revealed by Western blot analysis.

**Figure 5.** Expression of RUNX3 and claudin-1 in normal human gastric epithelium. Boxed regions are enlarged below. Specimens were counterstained with hematoxylin. Scale bars, 100  $\mu$ m.

**Figure 6.** Expression of RUNX3 and claudin-1 in human gastric cancer samples.

(A) Claudin-1-positive and RUNX3-positive gastric cancer samples. Intestinal and diffuse types are shown. Membranous claudin-1 and nuclear RUNX3 were detected.

(B) Claudin-1-negative and RUNX3-negative gastric cancer samples. Intestinal and diffuse types are shown. RUNX3 was retained in the cytoplasm in intestinal gastric cancer samples.

(C) The level of expression of claudin-1 was lower in RUNX3-negative samples than in RUNX3-positive samples. (i), (iv) and (vi) showed membranous staining of claudin-1. (ii), (iii) & (v) showed membranous and cytoplasmic staining of claudin-1. Specimens were counterstained with hematoxylin. Scale bars, 100  $\mu$ m.

**Table 1.** Expression of RUNX3 and claudin-1 in intestinal and diffuse types of gastric cancer

	RUNX3- negative/ claudin-1- negative n (%)	RUNX3- positive/ claudin-1- negative n (%)	RUNX3- negative/ claudin-1- positive n (%)	RUNX3- positive/ claudin-1- positive n (%)
Intestinal (n = 29)	9 (31%)	0 (0%)	15 (52%)	5 (17%)
Diffuse (n = 23)	8 (35%)	0 (0%)	5 (22%)	10 (43%)
Total (n = 52)	17 (33%)	0 (0%)	20 (38%)	15 (29%)

RUNX3-negative cases contain the cases showing cytoplasmic localization of RUNX3.

Figure 1.

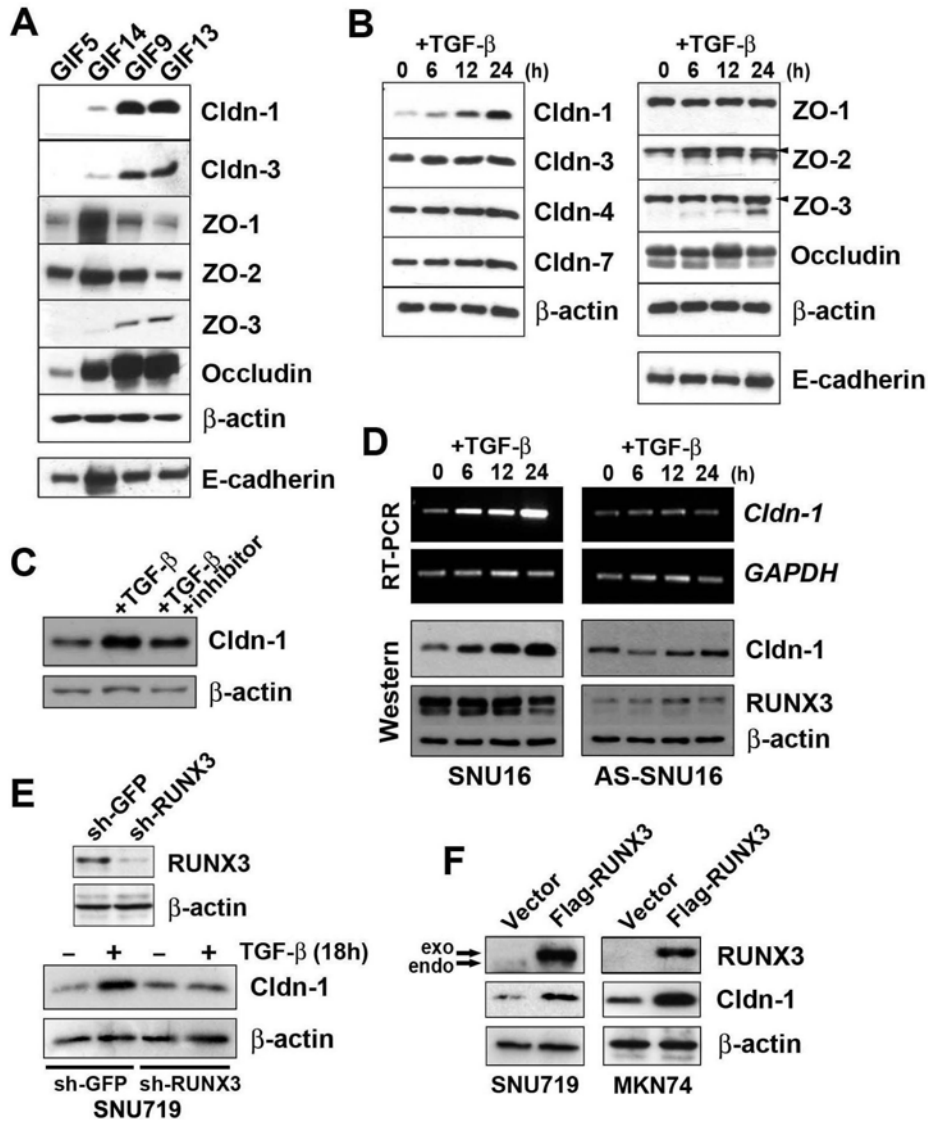


Figure 2.

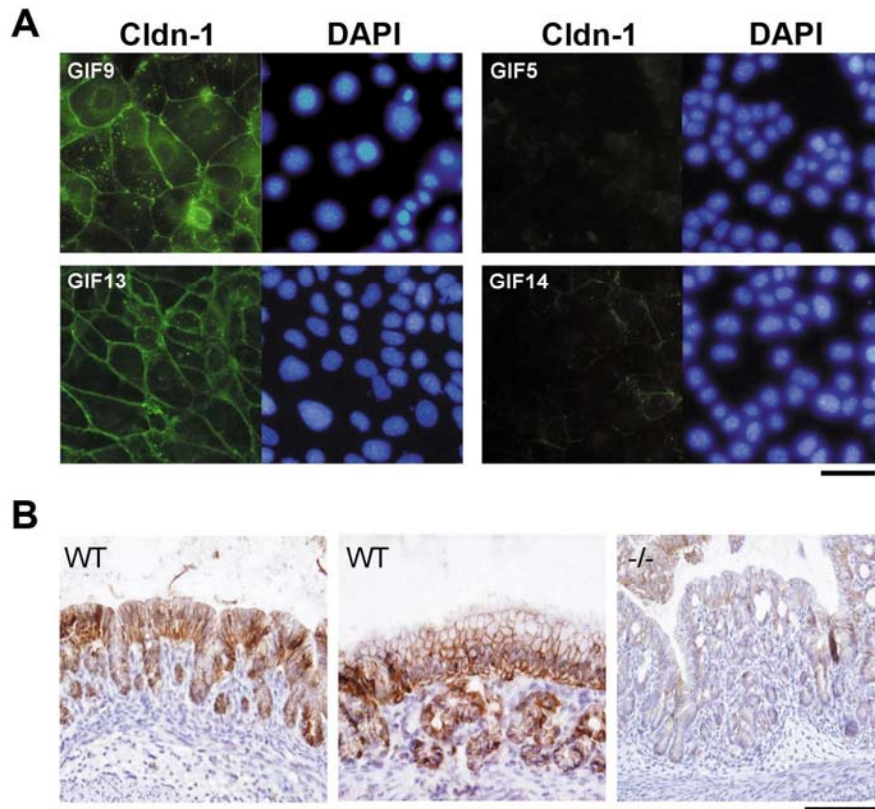






Figure 5.

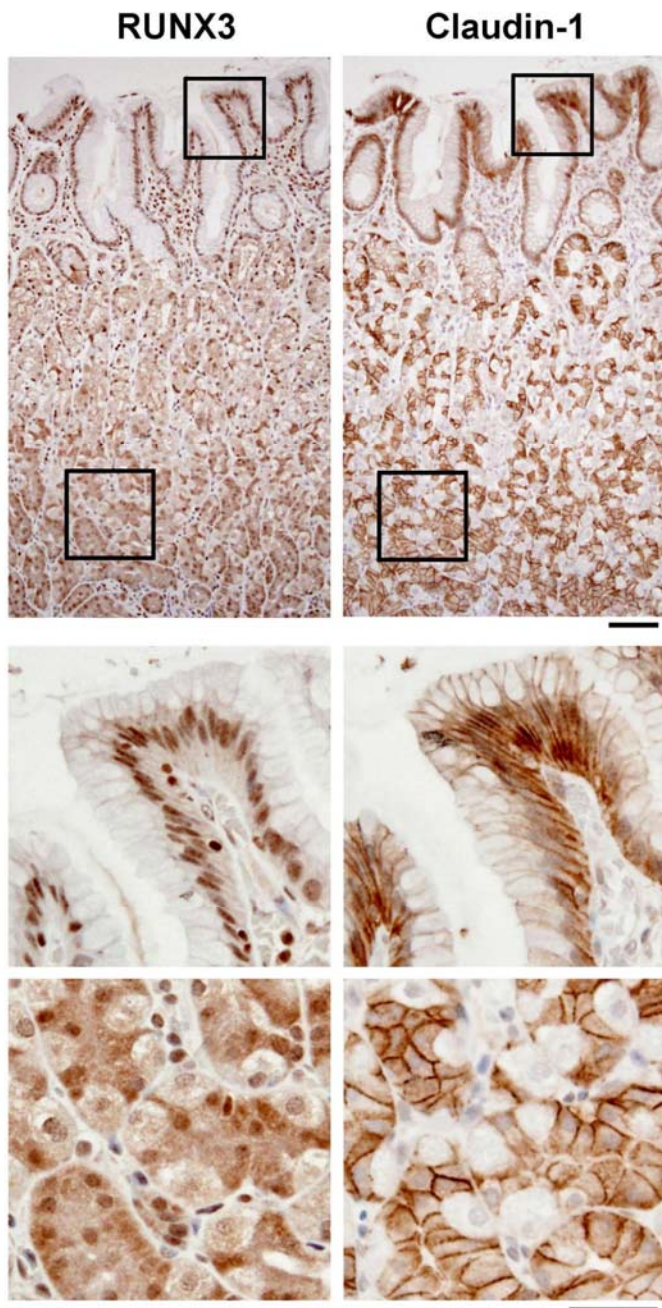
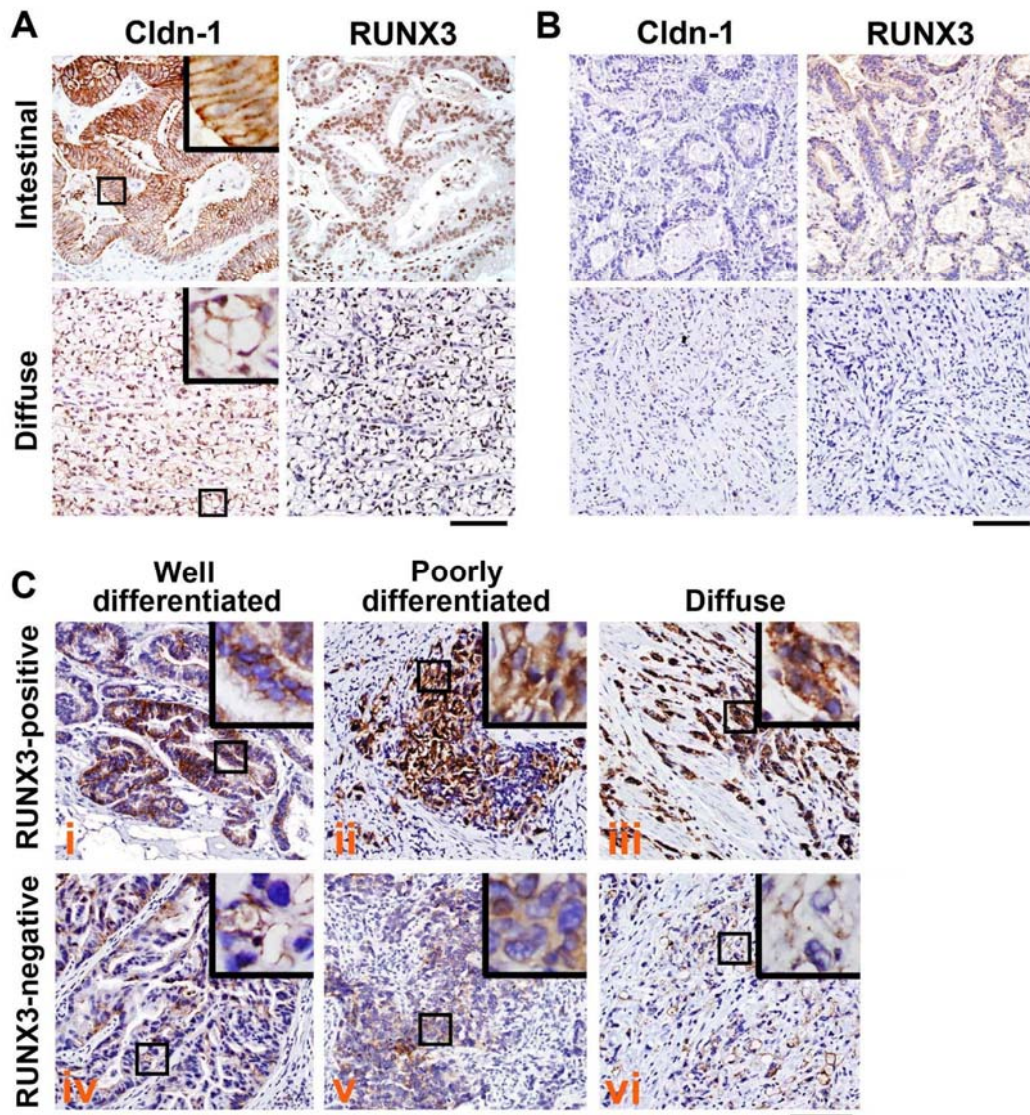


Figure 6.



**Supplementary Table 1.** Expression Profile of Genes Associated With Cell-Cell Adhesion in *Runx3*<sup>-/-</sup> GIF-5 vs *Runx3*<sup>+/+</sup> GIF-9 Cells, as Assessed by Oligonucleotide Microarray Analysis

Entrez gene ID	Gene symbol	Gene name	Ratio (GIF-5/GIF-9)
2802	Cldn1	Claudin-1	0.02
3188	Cldn1	Claudin-1	0.03
23812	Cldn3	Claudin-3	0.05
21894	Cldn4	Claudin-4	0.02
30129	Cldn6	Claudin-6	0.46
35973	Cldn7	Claudin-7	0.04
25782	Cldn9	Claudin-9	0.63
17740	Cldn12	Claudin-12	1.57
31760	Cldn14	Claudin-14	1.09
34226	Cldn15	Claudin-15	2.07
4033	Cldn18	Claudin-18	1.13
13904	Cldnd1	Claudin domain containing 1	1.05
28033	Cldnd1	Claudin domain containing 1	1.06
42954	Ocln	Occludin	0.53
43157	Ocln	Occludin	0.58

487	Jup	Junction plakoglobin	0.5
39262	Zfp120	Zinc finger protein 120	0.75
23540	Sympk	Symplekin	1.01
17415	Calr3	Calreticulin 3	4.3
8846	Calr	Calreticulin	0.51
8947	Calr	Calreticulin	0.65
13784	Cdk4	Cyclin-dependent kinase 4	0.85
24747	Cdk6	Cyclin-dependent kinase 6	1.58
25100	Cdk6	Cyclin-dependent kinase 6	1.51
25691	Cdk6	Cyclin-dependent kinase 6	2.14
3179	Jub	Ajuba	1.75
6774	Zyx	Zyxin	1.12
25825	Pxn	Paxillin	0.56
34015	Pxn	Paxillin	0.81
14888	Fhl2	Four and a half LIM domains 2	1.12
16769	Trip6	Thyroid hormone receptor interactor 6	0.92
4621	Trip6	Thyroid hormone receptor interactor 6	0.89
42961	Ash1	Ash1 (absent, small, or homeotic) like ( <i>Drosophila</i> )	0.7

218	Ash1	Ash1 (absent, small, or homeotic) like ( <i>Drosophila</i> )	0.6
12639	Ctnna1	Catenin (cadherin-associated protein), $\alpha$ 1	0.85
9543	Ctnna1	Catenin (cadherin-associated protein), $\alpha$ -like 1	0.44
29898	Ctnna1	Catenin (cadherin-associated protein), $\alpha$ -like 1	0.56
32399	Ctnna1	Catenin (cadherin-associated protein), $\alpha$ -like 1	0.92
34600	Ctnna1	Catenin (cadherin-associated protein), $\alpha$ -like 1	0.52
6845	Ctnnb1	Catenin (cadherin-associated protein), $\beta$ 1	1.16
7115	Ctnnb1	Catenin (cadherin-associated protein), $\beta$ 1	1.47
5128	Ctnnb1	Catenin (cadherin-associated protein), $\beta$ 1	1.11
13598	Ctnnb1	Catenin (cadherin-associated protein), $\beta$ 1	1.12
26926	Ctnnb1	Catenin (cadherin-associated protein), $\beta$ 1	1.13
30387	Ctnnb1	Catenin (cadherin-associated protein), $\beta$ 1	1.12
31524	Ctnnb1	Catenin (cadherin-associated protein), $\beta$ 1	1.13
33613	Ctnnb1	Catenin (cadherin-associated protein), $\beta$ 1	1.13
33796	Ctnnb1	Catenin (cadherin-associated protein), $\beta$ 1	1.11

35059	Ctnnb1	Catenin (cadherin-associated protein), $\beta$ 1	1.29
35625	Ctnnb1	Catenin (cadherin-associated protein), $\beta$ 1	1.17
36727	Ctnnb1	Catenin (cadherin-associated protein), $\beta$ 1	1.12
34740	Ctnnb11	Catenin (cadherin-associated protein), $\beta$ -like 1	1.05
35364	Ctnnb11	Catenin (cadherin-associated protein), $\beta$ -like 1	1.06
6957	Ctnnd1	Catenin (cadherin-associated protein), $\delta$ 1	1.06
7756	Ctnnd1	Catenin (cadherin-associated protein), $\delta$ 1	1.51
38639	Ctnnd1	Catenin (cadherin-associated protein), $\delta$ 1	1.94
7368	Ctnnbip1	Catenin $\beta$ interacting protein 1	0.91
188	Cdh1	Cadherin 1	0.78
4370	Cdh1	Cadherin 1	0.78
14130	Cdh1	Cadherin 1	0.82
20989	Cdh1	Cadherin 1	0.81
24570	Cdh1	Cadherin 1	0.81
28517	Cdh1	Cadherin 1	0.8
29329	Cdh1	Cadherin 1	0.8
33419	Cdh1	Cadherin 1	0.8

36281	Cdh1	Cadherin 1	0.81
41601	Cdh1	Cadherin 1	0.79
28937	Cdh3	Cadherin 3	0.08
13122	Cdh10	Cadherin 10	4.33
16804	Cdh11	Cadherin 11	0.55
14183	Cdh13	Cadherin 13	0.75
36584	Cdh17	Cadherin 17	2.89
9301	Itga2	Integrin $\alpha$ 2	0.98
7422	Itga2b	Integrin $\alpha$ 2b	0.41
11996	Itga3	Integrin $\alpha$ 3	0.38
28548	Itga3	Integrin $\alpha$ 3	0.34
40224	Itga3	Integrin $\alpha$ 3	0.39
32206	Itga4	Integrin $\alpha$ 4	1.85
16783	Itga5	Integrin $\alpha$ 5 (fibronectin receptor $\alpha$ )	1.72
5434	Itga6	Integrin $\alpha$ 6	1.82
9756	Itga6	Integrin $\alpha$ 6	1.55
28298	Itga6	Integrin $\alpha$ 6	1.4
1470	Itga7	Integrin $\alpha$ 7	0.36
20492	Itga7	Integrin $\alpha$ 7	0.31

36562	Itgae	Integrin, $\alpha$ E, epithelial associated	1.09
1127	Itgal	Integrin $\alpha$ L	1.25
15941	Itgav	Integrin $\alpha$ V	1.13
30803	Itgav	Integrin $\alpha$ V	1.18
3878	Itgb1	Integrin $\beta$ 1 (fibronectin receptor $\beta$ )	0.69
5038	Itgb1	Integrin $\beta$ 1 (fibronectin receptor $\beta$ )	0.8
6517	Itgb1	Integrin $\beta$ 1 (fibronectin receptor $\beta$ )	0.68
7627	Itgb1	Integrin $\beta$ 1 (fibronectin receptor $\beta$ )	0.71
15484	Itgb1	Integrin $\beta$ 1 (fibronectin receptor $\beta$ )	0.7
15683	Itgb1	Integrin $\beta$ 1 (fibronectin receptor $\beta$ )	0.69
25292	Itgb1	Integrin $\beta$ 1 (fibronectin receptor $\beta$ )	0.71
26331	Itgb1	Integrin $\beta$ 1 (fibronectin receptor $\beta$ )	0.72
29211	Itgb1	Integrin $\beta$ 1 (fibronectin receptor $\beta$ )	0.71
33166	Itgb1	Integrin $\beta$ 1 (fibronectin receptor $\beta$ )	0.69
33758	Itgb1	Integrin $\beta$ 1 (fibronectin receptor $\beta$ )	0.69
17200	Itgb1bp1	Integrin $\beta$ 1-binding protein 1	0.73
34448	Itgb1bp1	Integrin $\beta$ 1-binding protein 1	1.23
33120	Itgb2	Integrin $\beta$ 2	0.32

5839	Itgb3	Integrin $\beta$ 3	4.26
35332	Itgb3	Integrin $\beta$ 3	1.42
6271	Itgb3bp	Integrin $\beta$ 3-binding protein ( $\beta$ 3-endonexin)	2.12
6449	Itgb4	Integrin $\beta$ 4	0.23
12964	Itgb4	Integrin $\beta$ 4	0.23
28162	Itgb4	Integrin $\beta$ 4	1.23
16065	Itgb4bp	Integrin $\beta$ 4-binding protein	0.8
17137	Itgb4bp	Integrin $\beta$ 4-binding protein	0.9
26110	Itgb4bp	Integrin $\beta$ 4-binding protein	0.8
36438	Itgb5	Integrin $\beta$ 5	2.61
8658	Itgb6	Integrin $\beta$ 6	1.07
22943	Itgb6	Integrin $\beta$ 6	1.55
39766	Itgb6	Integrin $\beta$ 6	1.64
12531	Itgb7	Integrin $\beta$ 7	0.35
42875	Crb3	Crumbs homolog 3 ( <i>Drosophila</i> )	0.16
33819	Crb1	Crumbs homolog 1 ( <i>Drosophila</i> )	1.37
24656	Jam4	Junctional adhesion molecule 4	0.99
28942	Jam2	Junctional adhesion molecule 2	19.84

40749	Jam4	Junctional adhesion molecule 4	0.97
32468	L1cam	L1 cell adhesion molecule	0.17
38348	Vezt	Vezeatin, adherens junctions transmembrane protein	0.86
10279	Cdc42	Cell division cycle 42 homolog ( <i>Saccharomyces cerevisiae</i> )	1.07
15744	Cdc42	Cell division cycle 42 homolog ( <i>S cerevisiae</i> )	0.79
33085	Cdc42	Cell division cycle 42 homolog ( <i>S cerevisiae</i> )	1.12
6306	Cgn	Cingulin	0.91
22246	Cgn	Cingulin	0.64
34374	Cgn	Cingulin	0.64
32668	Dlg7	Discs, large homolog 7 ( <i>Drosophila</i> )	0.66
33705	Dlg7	Discs, large homolog 7 ( <i>Drosophila</i> )	0.56
35046	Dlg5	Discs, large homolog 5 ( <i>Drosophila</i> )	0.66
35772	Dlgh1	Discs, large homolog 1 ( <i>Drosophila</i> )	0.56
36439	Dlgh3	Discs, large homolog 3 ( <i>Drosophila</i> )	0.34
770	Dlgh1	Discs, large homolog 1 ( <i>Drosophila</i> )	0.43
7348	Dlg5	Discs, large homolog 5 ( <i>Drosophila</i> )	0.58
34455	Rab13	RAB13, member RAS oncogene family	0.58

17836	Dsp	Desmoplakin	0.83
23455	Dsp	Desmoplakin	0.82
36611	Dsp	Desmoplakin	0.87
21804	Vcl	Vinculin	0.41
25846	Vcl	Vinculin	0.56
5744	Tln1	Talin 1	0.85
10197	Tln1	Talin 1	0.74
12934	Tln2	Talin 2	0.44
14973	Tln2	Talin 2	0.47
27311	Tln1	Talin 1	0.94
40914	Ilk	Integrin-linked kinase	0.7
15769	Flna	Filamin, $\alpha$	0.42
25062	Flna	Filamin, $\alpha$	0.62
38232	Flna	Filamin, $\alpha$	0.37
406	Flnb	Filamin, $\beta$	0.68
2498	Flnb	Filamin, $\beta$	0.53
11971	Flnb	Filamin, $\beta$	0.57
13550	Flnb	Filamin, $\beta$	0.59
40558	Flnb	Filamin, $\beta$	0.6

2262	Flnc	Filamin c, $\gamma$ (actin-binding protein 280)	2.12
27334	Flnc	Filamin c, $\gamma$ (actin-binding protein 280)	2.07
30827	Flnc	Filamin c, $\gamma$ (actin-binding protein 280)	2.32

NOTE. Agilent Technologies (Santa Clara, CA) equipment was used for oligonucleotide microarray analysis.